agronomy

MDPI

Article

Soil Salinity Prediction Using Remotely Piloted Aircraft Systems under Semi-Arid Environments Irrigated with Salty Non-Conventional Water Resources

Francisco Pedrero Salcedo [1,*], Pedro Pérez Cutillas [2], Faissal Aziz [3,4], Marina Llobet Escabias [5], Harm Boesveld [5], Harm Bartholomeus [6] and Anas Tallou [4]

[1] Irrigation Department, Centro de Edafología y Biología Aplicada del Segura (CEBAS-CSIC) Apdo. 164, Espinardo, 30100 Murcia, Spain
[2] Department of Geography, Campus de La Merced, 30001 Murcia, Spain
[3] Laboratory of Water, Biodiversity & Climate Change, Semlalia Faculty of Sciences, Cadi Ayyad University, Marrakech 40000, Morocco
[4] National Centre for Research and Study on Water and Energy (CNEREE), Cadi Ayyad University, Marrakech 40000, Morocco
[5] Water Resources Management Group, Wageningen University & Research, Droevendaalsesteeg 4, 6708 PB Wageningen, The Netherlands
[6] Geo-Information Science and Remote Sensing, Wageningen University & Research, Droevendaalsesteeg 4, 6708 PB Wageningen, The Netherlands
* Correspondence: fpedrero@cebas.csic.es; Tel.: +34-665961041

Citation: Pedrero Salcedo, F.; Pérez Cutillas, P.; Aziz, F.; Llobet Escabias, M.; Boesveld, H.; Bartholomeus, H.; Tallou, A. Soil Salinity Prediction Using Remotely Piloted Aircraft Systems under Semi-Arid Environments Irrigated with Salty Non-Conventional Water Resources. *Agronomy* **2022**, *12*, 2022. https://doi.org/10.3390/agronomy12092022

Academic Editors: Victoriano Martínez-Alvarez, Belen Gallego-Elvira and Martín Eduardo Espósito

Received: 1 July 2022
Accepted: 22 August 2022
Published: 26 August 2022

Abstract: The effects of climate change on food security have been unfavorable, particularly in the area of Murcia where there is a water shortage. To satisfy crop needs, farmers combine several irrigation water sources, such as brackish groundwater, desalinated water, reclaimed water, and desalinated water. Good agricultural and irrigation practices are essential for preventing soil salinization and production losses, and remote sensing might be used to evaluate these practices. This research, performed in an experimental field under greenhouse conditions and in an open-air commercial lettuce field irrigated with non-conventional water sources, determined that the Salinity Index (SI) applied to bare soil is a useful spectral index, providing an R^2 range of 0.40 to 0.83. The other metric used to the bare soil, the Normalized Difference Salinity Index (NDSI), exhibited poor correlations, with R^2 values as high as 0.49. Moreover, the thermal camera did not operate well within the greenhouse, but it performed in the commercial plot, where the canopy temperature was linearly correlated, with an R^2 value of 0.50. The second analyzed vegetative metric, the Normalized Difference Plants Index (NDVI), was exclusively applied to the vegetation and showed minimal relationships with the soil salinity. In the visual evaluation of the maps, the temperature patterns of the canopy were strikingly comparable to the electrical conductivity of the soil, which was not the case for the other analyzed indices. The use of non-conventional moderately saline irrigation water sources negatively impacts the lettuce development by decreasing the fresh head weight and increasing the sodium and chloride leaf concentrations.

Keywords: wastewater treatment; remote sensing; water reuse; reclaimed water; multispectral images; precision agriculture; unmanned aerial vehicle

1. Introduction

The effects of climate change on food security, desertification, and land degradation are negative. Considering the forecasted population expansion, which is projected to reach 10 billion people by 2050 [1], and the decline in land and water available for agriculture, it would be difficult to meet the food demands in the future.

Reclaimed water has become one of the most appealing and cost-effective non-conventional water sources for agriculture [2], irrigating 20 million hectares globally [3]. It

has boosted global food security in several regions [4]. However, the requirements and severe laws for using reclaimed water may be barriers to this practice in certain countries [5], since only 41% of the treated waste water is utilized for irrigation [5,6].

Utilizing recycled water in agriculture has several benefits. One of them is lowering the reliance on traditional water sources, such as rivers and aquifers [7–9], which is crucial in arid and semi-arid regions that are already experiencing water shortages. In addition, as a source of macronutrients and micronutrients, it minimizes the need for synthetic fertilizers [7–9]. In addition, the use of reclaimed water in agriculture minimizes the discharge of contaminants into the environment [10–13], since it is preferable to direct the dumping into water bodies [7,9,14].

Despite the fact that the use of recycled water in agriculture has certain benefits, there are also downsides and hazards. For example, the introduction of viruses and heavy metals into the food chain may result in health issues and monetary repercussions [5,15]. Due to the buildup of salts, which may increase the soil salinity and soil sodicity and decrease the soil permeability, the soils may be harmed [7,10,14]. Together with the buildup of heavy metals, this decreases agricultural production [10].

Precision agriculture is centered on applying the appropriate quantity of inputs at the appropriate time and location [15]. This is possible, for example, with the data supplied by remote sensing, using satellite photos, aircraft, and RPAS (remotely piloted aircraft systems) to identify and monitor crop and soil physical parameters. This non-destructive approach permits the collection of accurate data without directly damaging the crops, playing a crucial role in the development of precision agriculture that is more efficient, productive, and sustainable. In the agricultural sector, remote sensing has several uses, including irrigation monitoring and management, soil mapping, crop nutrient shortage diagnosis, crop yield forecasts, soil moisture measurements, and insect and disease identification [16,17].

In recent years, soil salinity assessments using remote sensing have been extensively studied for modeling and mapping soil salinity on a large scale in various countries [18–24]. Thermal imagery has been used to evaluate various parameters, including water changes [24,25] and the effects of salinity in soilless culture to estimate the leaf area index values and to improve irrigation management practices [25]. However, the application of this method to evaluate the soil salinity has received little research. Using satellite images, some researchers [26,27] found strong connections between the canopy temperature and plant salinity stress in Australia and Uzbekistan at a broad scale. In addition, at the field level, researchers [26,28] have established strong correlations in alfalfa fields using thermal infrared remote technology and in quinoa fields using RPAS imaging, respectively.

Due to a lack of water, Murcia (Spain) has relied on salty non-conventional water supplies to cover all of its irrigation needs, which may increase the soil salinity and degrade the agricultural yield and quality [12,17]. The use of RPAS thermography with multispectral imaging is a promising method for assessing soil salinity. These remote sensing approaches might improve the spatial and temporal accuracy of soil salinity evaluations and save farmers time and money [16].

The aim of this study is to evaluate the soil salinity and lettuce growth in Murcia using non-conventional saline water supplies in a greenhouse experimental field and in an open air commercial plot. In the experimental plot, the irrigation water will come from the DESERT prototype, while in the commercial plot a mixture of different irrigation water sources will be used. To assess the effects of the irrigation, thermal and multispectral images collected by RPAS will be analyzed.

2. Materials and Methods

2.1. Experimental Setup

The study was carried out in a greenhouse located on a research platform from CEBAS-CSIC in the Balsicas, Roldan, and Lo Ferro municipal wastewater treatment plant (WWTP) in the Murcia region (southeastern Spain). The greenhouse characteristics during

the experiment were the average temperature, surface area, relative air humidity, and transpiration at 15 °C, 680 m^2, 67%, and 0.5 Lm^{-2}, respectively.

2.2. Experimental Plot (Greenhouse)

The experiment included the soil cultivation of 121 m^2 of mini-Romaine lettuce (*Lactica Sativa* var. *romanica*) of the new Atómicos variety from the company Gautier. The transplantation occurred on 24 October 2019, and the harvesting occurred on 16 December 2019. The spacing between ridges on the same ridge was 15 cm, and the plantation frame was 0.167 × 1 m. Therefore, the planting density was six plants per square meter. The plot was irrigated with the reclaimed water produced in the DESERT prototype, which from a secondary effluent of the WWTP generated non-saline water (EC = 0.7–0.8 dS/m) that was used to irrigate the CP (control plot) and moderately saline water (with an EC of 3–4 dS/m) that was used to irrigate the SP (saline plot). The irrigation system comprised six driplines in the center of each ridge with a diameter of 16 mm, a thickness of 1 mm, a spacing of 33 cm, and a flow rate of 2.20 l/h at a pressure of 3.5 bar. A volumetric counter was set at the beginning of each drip line to determine the quantity of irrigation water supplied.

2.3. Commercial Plot (Open-Air)

The commercial plot contained 1.17 hectares of lettuce (variety Mestiza). The planting took place on 17 October 2019, with a density of 6.75 lettuce plants per square meter, and the harvest occurred on 6 January 2020. The irrigation water was applied by drip irrigation (flow 4 L h^{-1}) and provided by an irrigation community, and was a mix of different conventional and non-conventional sources: Tajo-Segura water transfer (88.7%), the Segura river basin (3.0%), reclaimed water from WWTPs (6.7%), and the Mojon desalination plant (1.6%).

2.4. Soil Analysis

2.4.1. Soil Sample in the Experimental Plot

The soil analysis was conducted by collecting samples from various plot areas. Before planting (T0), 19 days after transplantation (T1), 39 days after transplantation (T2), and before harvesting (T3), soil samples were collected from the experimental plot at various intervals (T3). Nine soil samples were collected in T0 to describe the soil. In T1 and T2, a total of 24 samples were collected, two in each row. In T3, eleven more samples were collected between the ridges.

2.4.2. Soil Sample in the Commercial Plot

Due to the extended growing season, more samples were gathered from the commercial plot. The first soil sample was taken on the day of transplanting (T0), and the next five measurements were taken every 15 days (T1, T2, T3, T4). Each time, a total of 12 soil samples were collected randomly at depths of 0.2 m and 0.3 m away from the emitter.

After collecting the soil samples, they were taken to the laboratory for analysis. Initially, the samples were baked for at least 24 h at 100 °C. Then, a 2-mm-mesh sieve was used to filter the soil and prepare it for analysis. Nine soil samples were collected in order to describe the soil. In T1 and T2, a total of 24 samples were collected, two from each row. In T3, eleven more samples were collected between the ridges.

2.4.3. Soil Salinity and Saturated Soil Paste (SSP)

The electrical conductivity (EC) of the soil could be used to evaluate the soil's salinity. The calculated value indicates the salts present in the soil, which, if excessive, might have a detrimental effect on crop development. In this experiment, the saturated soil paste (SSP) technique was used to determine the electrical conductivity (EC) of the soil.

The SSP method was used to determine the soil's EC because it provides an accurate estimate of the total soluble salts in the soil [28]. Into a 100 mL plastic cup, roughly 80 g of dirt was placed. Then, distillated water was added to soak the soil. The mixture was stirred

using a stirring stick to prevent lumps. The Eutech PC2700 was used to assess the EC of the soil saturation (ECsat). In addition, a map of the ECsat was generated using ArcGIS (version 10.5) using the IDW tool to extrapolate the sample values to the whole field.

2.4.4. Soil pH

The pH of the soil was determined by extracting soil and water at a ratio of 1:2.5. In a tiny cup, 10 g of dirt and 25 milliliters of distilled water were combined. The samples were then stirred using a Velp Scientifica magnetic stirrer for 30 to 45 min, after which the pH was measured with a Eutech PC 2700 instrument while the sample was being stirred with the Velp Scientifica magnetic stirrer. In addition, a pH map was generated using ArcGIS (version 10.5) using the IDW tool to extrapolate the sample values to the whole area.

2.4.5. Mineral Contents of the Soil and the Irrigation Water

The soil mineral contents were determined using a 1:5 soil extract. This approach requires a ratio of 1:5 between the dirt and water. In the experiment, 20 g of dirt and 100 g of distilled water were measured and combined. After two hours of shaking to dissolve the soil salts into the water, the samples were centrifuged at 4000 rpm for ten minutes in an Ortoalresa Unicen 21 system. Using a syringe, the fluid portion was extracted from the cups and filtered using 0.45-um-sized Chromafil® Xtra PET-45/25 filters. The soil and irrigation water solutions were then transported to a laboratory for mineral analysis to identify anions (F^-, Cl^-, $NO_2{}^-$, Br^-, $NO_3{}^-$, $PO_4{}^{3-}$, and $SO_4{}^{2-}$) and cations (Al^{3+}, As^{3+}, Be^{2+}, Bi^{2+}, B^{3+}, Ca^{2+}, Cd^{2+}, Co^{2+}, Cr^{2+}, Cu^{2+}, Fe^{2+}, K^+, La^{3+}, Li^+, Mg^{2+}, Mn^{2+}, Mo, Na^+, Ni^{2+}, Pb^{4+}, P, Rb+, Sb^{3+}, Sr^{2+}, Ti^{3+}, Tl^+, V^{3+}, and Zn^{2+}). In the experimental plot, samples of irrigation water were collected from two tanks, one containing salty irrigation water and the other containing non-saline irrigation water generated by the DESERT prototype. They were collected from the farmer's water pond for the commercial plot. For the physicochemical analyses, the different types of irrigation water were grab-sampled biweekly during the experimental period in clean, non-sterile bottles (not intended for microbiological analyses) that were first rinsed and filled with the corresponding water. Once transported to the lab, the samples were stored at 5 °C before processing. The macronutrients ($NO_3{}^-$, $PO_4{}^{3-}$, K, Ca, Mg), micronutrients (Fe, Mn, Zn, Cu), phytotoxic elements (B, Cl^-, Na), and metals were analyzed by mass spectrometry, using an inductively coupled plasma spectrometer (ICP-ICAP 6500 DUO Thermo, England), and by ion chromatography, using a chromatograph (Metrohm, Switzerland). The samples used for both the spectrometry and chromatography were previously filtered using 45 mm filters and stored in 10 mL test tubes. The EC and pH values were measured with a Eutech PC 2700 multi-parameter instrument (Eutech Instruments, Singapore).

2.5. Crop Analysis

2.5.1. Lettuce Samples in the Experimental and Commercial Plots

In trials T1, T2, and T3, a total of 12 lettuces were randomly selected from each row to determine their mineral content. In addition, 20 lettuces were utilized in T3 to determine the following characteristics: fresh weight of the whole lettuce, fresh weight of the head lettuce, head diameter, and head height.

To determine the mineral content of the leaves, four random lettuces from the commercial plot were harvested at T3 and T4 and five at harvest. In addition, 10 lettuces were harvested in order to determine the fresh weight of a head of lettuce, the circumference, and the height.

2.5.2. Mineral Content of the Leaves

The mineral content of the leaves was determined using the following procedures. First, the samples were placed in an oven at 60 °C for at least 48 h to fully dry the leaves. Then, the leaves were ground into a fine powder. Next, 0.1 g of leaves was combined with 40 milliliters of distilled water and shaken for 10 min. The samples were next filtered using

gauze, followed by a Chromafil® Xtra PET-45/25 filter. The N, C, anions (F^-, Cl^-, $NO_2{}^-$, Br^-, $NO_3{}^-$, $PO_4{}^{3-}$, and $SO_4{}^{2-}$), and cations were measured using the leaf extract that was delivered to the laboratory (Al^{3+}, As^{3+}, Be^{2+}, Bi^{2+}, B^{3+}, Ca^{2+}, Cd^{2+}, Co^{2+}, Cr^{2+}, Cu^{2+}, Fe^{2+}, K^+, La^{3+}, Li^+, Mg^{2+}, Mn^{2+}, Mo, Na^+, Ni^{2+}, Pb^{4+}, P, Rb+, Sb^{3+}, Sr^{2+}, Ti^{3+}, Tl^+, V^{3+}, and Zn^{2+}).

2.6. Remote Sensing Techniques

2.6.1. Data Collection and Image Processing

The spectral and thermal responses of the soil and canopy to salinity were measured using RPAS imagery. The MicaSense RedEdge-M multispectral camera and the FLIR ZENMUSE XT2 thermal camera were utilized (green (G), blue (B), near infrared (*NIR*), red (R), and red edge (R) (RE)). Additionally, two thermal maps were obtained for the commercial plot, and a thermal video was given for the experimental plot. On each plot, a total of three flights were conducted using a different RPAS or a stick to support the camera.

ArcGIS (version 10.5) was used to analyze the imagery and to produce two vegetative and soil indices, which were applied to determine their relationship with the soil salinity. The vegetative ones included the well-known Normalized Difference Vegetation Index (*NDVI*), which offers information on the greenness and biomass, and the canopy temperature, since one of the responses of plants to salt stress is stomatal closure, which raises the leaf temperature [15]. In prior research, the most recent indices demonstrated strong connections with soil salinity [26–28]. The Salinity Index (SI) and Normalized Difference Salinity Index (*NDSI*), which give information on the soil salinity, were selected from the soil indices. In addition, the ECsat data received from field measurements was included and interpolated using the inverse distance weighted (IDW) technique to generate raster layers from points [15]. The *NDVI* and canopy temperature were only applied to the vegetative area, whereas the *SI* and *NDSI* were only applied to the bare soil. The formulas for the *SI*, *NDVI,* and *NDSI* are presented below:

$$SI = \sqrt{G * R} \quad (1)$$

$$NDVI = \frac{(NIT - RER)}{(NIR + RED)} \quad (2)$$

$$NDSI = \frac{(Green - SWIR)}{(Green + SWIR)} \quad (3)$$

2.6.2. Correlation of ECsat with the Indices

The Pearson correlations between the ECsat and spectral indices were calculated using the PAST statistical package [29]. The values of the vegetative indices, canopy Ta, and *NDVI* were acquired using ArcMap 10.5 to calculate the average pixel value of the vegetation on top of the soil sample or the nearest one. For the indices applied to bare soil, the SI and *NDSI*, the average of the pixel values closest to the site of the soil sample from which the ECsat was derived was utilized. The associations between the various examined indices and the soil salinity were determined using the coefficient of determination, R^2.

3. Results

3.1. Crop Development in Greenhouse Plots

3.1.1. Visual Assessment and Lettuce Characteristics

The salts in the soil impacted the crop growth from the beginning. The CP lettuces grew faster and healthier than the SP lettuces. The T1 sample in CP had a larger diameter, more leaves, and larger leaves than in SP. The T2 sample's height and diameter were comparable, but the CP sample's heart was greater. Some lettuces were removed because Sclerotinia sclerotiorum began rotting the neck and melted the lettuces. The salts burnt and wrinkled several leaves. In T3, right before harvesting, the impacts of the salts were clear because the lettuce in the SP was shorter, wrinkled, and had burnt tips. In CP, the

lettuces were healthy. Before harvesting the experimental plot, the lettuce dry weight in T1 was 44.27% and in T2 it was 31.65%. The fresh weight of the entire lettuce in the CP was 26.24% greater, the head weight was 18.72% higher, and the dry weight of the heart was 9.26% higher than in the SP. The CP heart height and diameter were 1.11% and 3.40% greater than in the SP, respectively. The SP had 0.6% more water than the CP. The average dry wight of lettuce (g) in the CP was higher than in the SP in T1, T2, and T3. In addition, the whole lettuce weight (g), head lettuce weight (g), head lettuce height (cm), and head lettuce diameter (cm) at the harvesting stage in the CP were higher than in the SP. The results are illustrated in Table 1.

Table 1. Average dry weight and characteristics of the whole lettuce in T1 and T2, and of the lettuce head and the water content in T3 for the control plot (CP) and the saline plot (SP).

	Plot	Average Dry Weight of Lettuce (g)	Plot	Whole Lettuce Weight (g)	Head Lettuce Weight (g)	Height Lettuce Head (cm)	Head Lettuce Diameter (cm)
T1	**SP**	1.80 ± 0.48	**CP**	630.43 ± 96.20	379.53 ± 54.30	22 83 ± 0.85	11.40 ± 0 50
	CP	2.60 ± 0.13					
T2	**SP**	10.03 ± 1.85					
	CP	13.20 ± 1.53	**SP**	499.40 ± 76.72	319.70 ± 50.29	22.58 0.91	11.03 ± 0.57
T3	**SP**	7.34 ± 0.68					
	CP	8.02 ± 1.44					

3.1.2. Chemical Composition of the Irrigation Water in the Commercial Plot and Greenhouse

The irrigation water in the commercial plot had a very stable ECw, pH, and mineral content (Table 2) during the whole growing season, even though the farmer mixed different irrigation water sources. The average pH was 8.50 ± 0.43, and the ECw was 1.01 ± 0.11 dS/m, which made it slightly saline irrigation water. The irrigation water had a stable pH, with an average of 8.02 ± 0.13 in the CP and of 7.77 ± 0.15 in the SP. However, the ECw fluctuated during the first two samples that were taken. The average ECw during the growing season in the CP was 1 ± 0.38 dS/m and in the SP was 4.42 ± 0.41 dS/m, being slightly saline and moderately saline irrigation waters, respectively. The main differences in mineral contents between CW and SW can be seen. The highest differences in content were for Na^+, SO_4^{2-}, Cl^-, PO_4^{3-}, and Br^-. The sodium was 400% higher in the SP than in the CW, the sulphate ion was 246.32% higher, the chloride was 167.33% higher, the phosphate ion was 174.97% higher, and the bromine was 55.61% higher. Other elements such as the phosphate, sulfur, and nitrate ion contents showed lower differences, being higher in the SW by 20–30% than in CW.

Table 2. Chemical composition of the irrigation water compared to the control water.

Mineral Content (mg/L)	CW	SW	Irrigation Water (Greenhouse)
Cl^-	322.11 ± 368.19	861.10 ± 361.60	176.67 ± 21.42
Br^-	3.66 ± 2.76	7.89 ± 8.09	-
NO^{3-}	20.14 ± 6.47	25.71 ± 1.98	2.73 ± 0.64
PO_4^{3-}	3.94 ± 0.68	10.83 ± 7.85	3.18 ± 0.90
SO_4^{2-}	92.14 ± 63.37	319.10 ± 185.27	82.96 ± 17.05
Na^+	152.36 ± 43.50	762.63 ± 47.41	127.42 ± 13.08
P	1.37 ± 0.56	5.04 ± 4.09	1.00 ± 0.48
S	43.22 ± 19.76	149.86 ± 96.94	33.55 ± 10.49

3.1.3. Mineral Content of Leaves

The mineral composition of the leaves evolved through time, and certain variances existed between the CP and the SP (Table 3). The biggest difference was in the chloride and salt levels, with the SP lettuces having 95.77% and 67.35% higher rates than the CP at the conclusion of the growth season, respectively. Furthermore, the nitrogen difference was obvious, with larger levels in the SP, although the carbon content was identical in both plots. Finally, the calcium and iron concentrations in T3 were lower in the SP than in the CP.

Table 3. Mineral content of dried leaves in the control (CP) and saline (SP) plots (SP). T1 and T2 include the mineral content of the whole lettuce, but T3 solely contains the mineral content of the lettuce head.

Mineral	T1		T2		T3	
	CP	SP	CP	SP	CP	SP
N total (g/Kg dw)	49.03	50.95	39.40	43.42	38.73	45.75
C total (g/Kg dw)	370.66	373.53	340.24	350.65	393.07	393.96
Ca^{2+} (g/Kg dw)	16.67	17.56	25.85	19.56	7.41	5.81
Fe^{2+} (mg/Kg dw)	748.71	756.64	1326.60	887.33	103.52	66.20
Cl^- (mg/L)	144.25	150.69	150.15	194.27	62.36	122.08
Na^+ (g/Kg dw)	9.20	12.57	9.74	15.74	6.77	11.34

3.1.4. Salts in the Soil

The ECsat was moderately saline in T0 (before to transplantation), with an average value of 7.04 ± 0.82 dS/m. After some watering, T1 became slightly saline, with averages of 2.97 and 3.49 dS/m in the SP and CP, respectively. When compared to T1, the ECsat rose by 89.74% in the SP and by 24.1% in the CP in T2. Finally, samples were obtained on the ridges and between them (where there was no vegetation) before harvesting (T3) to examine whether there was a difference. The salt concentration between the lines was greater, as predicted, with values of about 8.5 dS/m in both fields, indicating that the lines were extremely saline. The SP ridges exhibited comparable values to T2, and the salinity in the CP fell to 2.70 dS/m. Figure 1 depicts the maps of the soil electrical conductivity (ECsat).

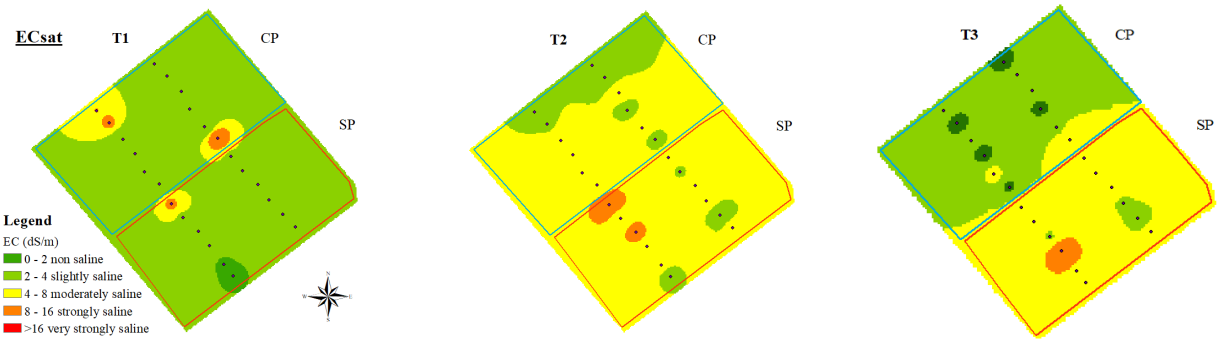

Figure 1. Maps of the electrical conductivity of the soil (ECsat) for the samples taken in the ridges (represented by black dots in the maps) in T1, T2, and T3.

3.1.5. Canopy Temperature

The canopy Temperature had negligible correlations in T2 and T3, with contradicting results between both samples. In T2, the temperaturein the SP had an average value of 25.2 ± 2.0 °C, while in the CP it was 23.8 ± 1.0 °C. When plants are under stress conditions, the leaf temperature increases due to a reduction in transpiration, which did not seem to occur in T3, where the average canopy temperature of the CP (17.4 ± 0.6 °C) was higher than in the SP (15.0 ± 1.5 °C) (Figure 2).

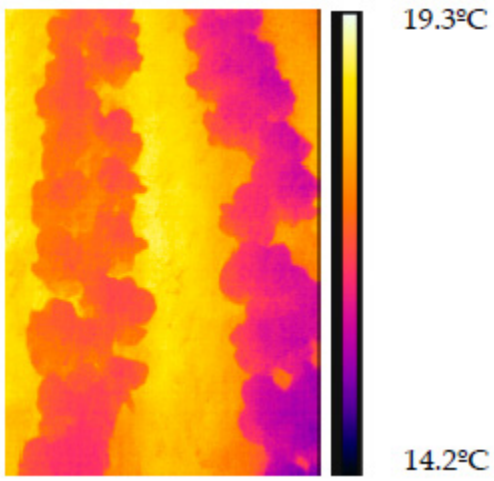

Figure 2. Thermal image examined using FLIR Tools to illustrate temperature variations between the SP row on the right and the CP row on the left in T3.

3.1.6. Normalized Difference Vegetation Index (NDVI)

The correlation between the ECsat and NDVI was insignificant for T1, T2, and T3, with an average R^2 of 0.02 for the whole dataset. This can also be seen in the maps (Figure 3), since the values of this vegetative index are fairly homogeneous over the whole field and do not seem to be related to the EC values of the soil, despite the fact that the NDVI values tend to drop as the ECsat values rise. As predicted, the NDVI climbed from T1 to T2, when it attained the greatest average, and then subsequently dropped somewhat before harvesting. The disparities between the SP and the CP were most noticeable in the early phases, when the average NDVI in T1 for the SP was 0.75 and for the CP was 0.8. Then, there was almost no difference between T2 and T3, with average values of 0.87 and 0.83, respectively.

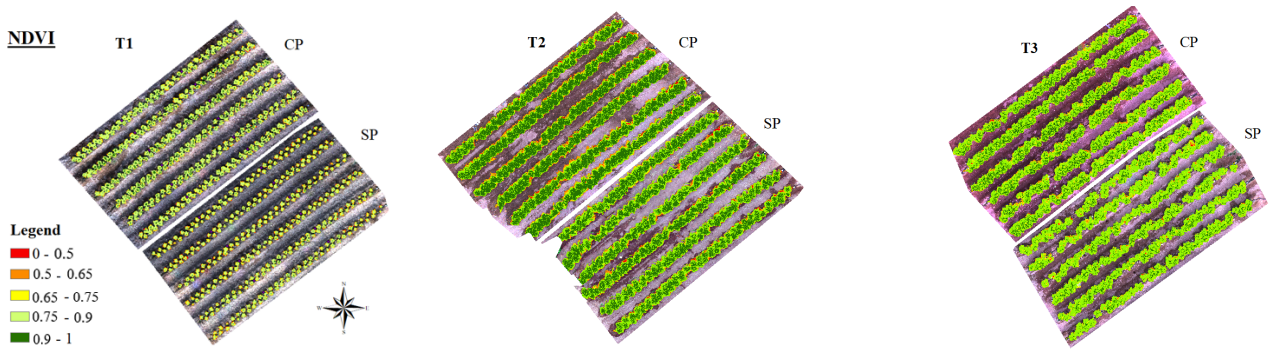

Figure 3. Maps of the NDVI applied to vegetation for T1, T2, and T3.

3.1.7. Salinity Index (SI)

Although the correlation between the SI and ECsat was almost zero for the whole dataset, there were strong positive correlations for T1, T2, and T3 and a moderate positive correlation for the samples obtained in T3 between the ridges. The greater the SI value, the higher the ECsat. The values in T2 and T3 were relatively close, while the SI in T1 was twice as high (or even higher) for the same soil salinity. As a result, the maps in Figure 4 show how many red and yellow areas there are in T1 compared to T2 and T3. The SI value has the opposite tendency to decline as the ECsat computed in the field. The various SI values between the ridges, which have greater values in the bottom half, may also be extracted from the maps. This was also seen in T3 samples collected between the ridges, which had greater salinity than the ridges. Except for the values from T1, which did not follow the same trend as the other values, the correlation of the remainder of the dataset with the equation was substantially positive (R2 = 0.82): EC_sat = (SI − 0.0401)/0.012.

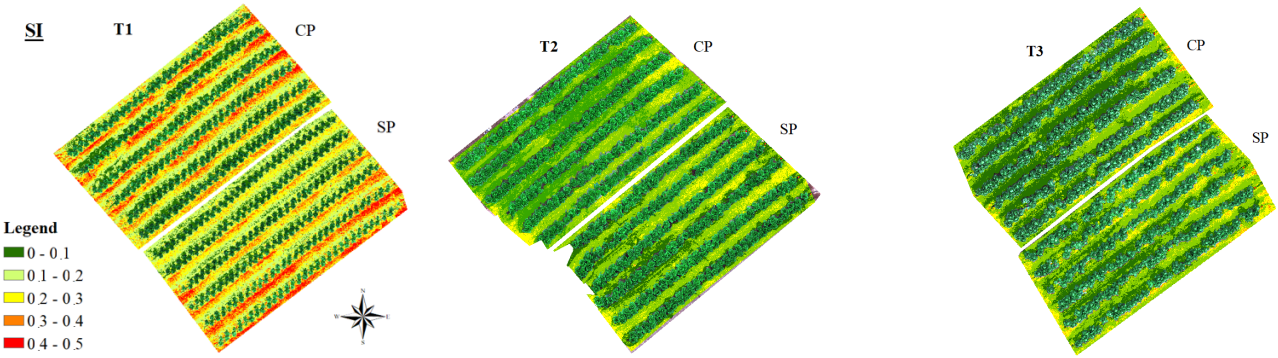

Figure 4. SI maps applied only to bare soil for T1, T2, and T3.

3.1.8. Normalized Difference Salinity Index (NDSI)

In T1 and T2, the NDSI had low correlations with the ECsat, but there was a substantial positive association in T3. The greater the NDSI, the higher the ECsat should be. The T1 values were higher than the T2 and T3 values (Figure 5). Excluding the T1 values, the dataset's correlation was virtually moderate, with an R^2 of 0.49 using the equation:

$$ECsat = \frac{(NDSI + 0.5524)}{0.0289} \quad (4)$$

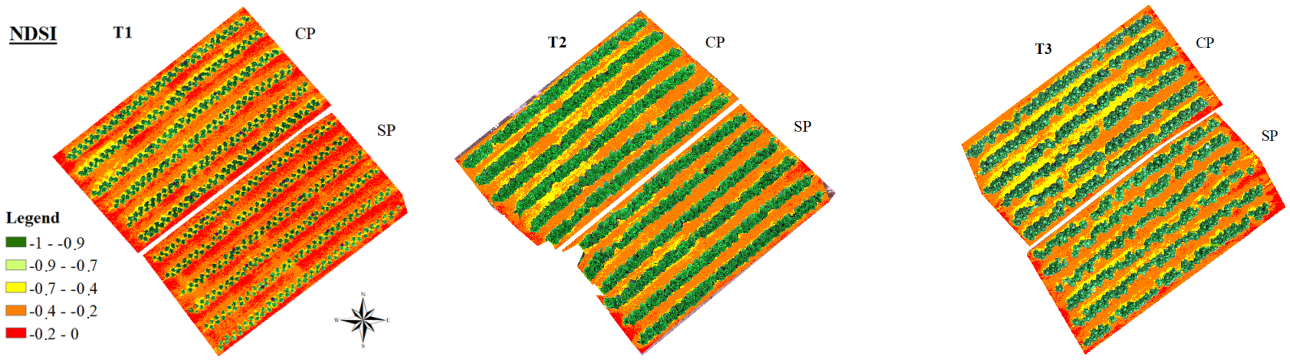

Figure 5. NDSI maps applied to bare soil for T1, T2, and T3.

In both plots, the average NDSI dropped throughout time, with a CP value of −0.30 in T1, −0.35 in T2, and −0.37 in T3. The SP had somewhat higher values of −0.26 in T1, −0.31 in T2, and −0.32 in T3. The slopes between T1 and T2 in both the CP and the SP were substantially larger than the slopes between T2 and T3.

3.2. Crop Development in Commercial Plot

3.2.1. Lettuce Weight and Mineral Content of Leaves

When harvested, the lettuces in the commercial plot had an average dry weight of 11.14 g and a water content of 97.02%. Furthermore, the average head diameter was 11.25 cm, and the average height was 23.73 cm. The mineral composition of leaves in the commercial plot remained stable throughout the growth season, with small exceptions of a few minerals (Table 4).

Table 4. Mineral contents of the dry leaves in the commercial plot for the whole lettuce in T3 and T4 and of the head lettuce at harvesting time.

Mineral	T3	T4	Harvesting
N total (g/Kg dw)	43.87	44.03	37.09
C total (g/Kg dw)	396.29	349.40	391.58
Ca^{2+} (g/Kg dw)	1.26	1.88	1.52
Cl^{-} (mg/L)	234.88	234.88	98.67
Fe^{2+} (mg/Kg dw)	1084.86	1308.56	1068.58
Mg^{2+} (g/Kg dw)	3.20	4.01	3.86

3.2.2. ECsat and DEM of the Plot

The average ECsat of the soil varied during the growth season, with a strong relationship with the rainfall. When sowing began in T0, the ECsat was high, since there had been little rain for more than a month. The salts were leached in T1 owing to the 28 mm of precipitation. There was little rain between T2 and T3, and the salts collected in the soil. Then, in T4, there was some rain before and after the samples were collected, resulting in a low ECsat value. Finally, the majority of the salts in T4 were leached owing to two days of precipitation that totaled 72.3 mm. The variations in the ECsat can be seen clearly in the maps in Figure 6, as can the salts' propensity to collect in the lowest half of the field (Figure 7).

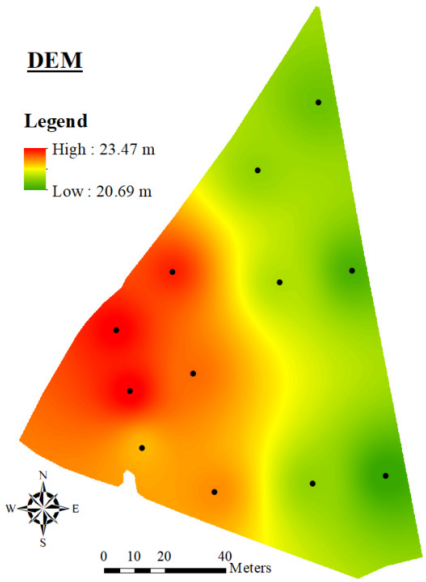

Figure 6. Digital elevation model (DEM) of the commercial field with the locations of the elevations marked with black dots.

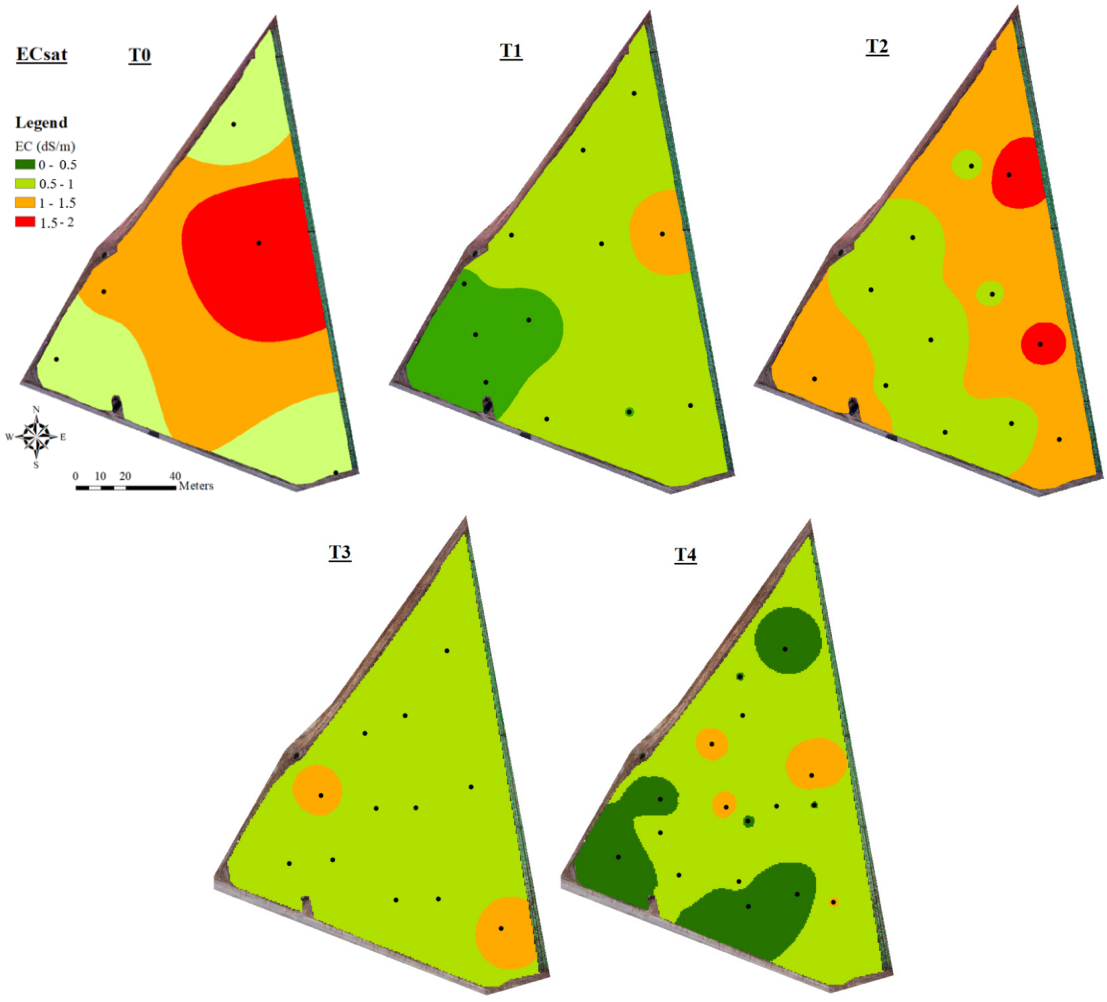

Figure 7. Maps showing the electrical conductivity of the soil (ECsat) for samples from T0, T1, T2, T3, and T4, with black dots indicating the positions of the soil samples.

3.3. Index Maps and Correlations with ECsat

3.3.1. Canopy Temperature

The canopy temperature had a moderate positive R^2 correlation in T2 of 0.5, while in T1 and for the entire dataset it was negligible (R^2 = 0.0). The higher correlation obtained in T2 was mainly because there were two samples with a much higher ECsat, and as two groups in the dataset can be distinguished, T2 and T4 (excluding the two high values), the correlation may not hold for a larger dataset. Looking at the thermal maps (Figure 8), it can be seen that for T2 the pattern of the temperatures is very similar to the one for the ECsat values, showing higher temperatures in the eastern part of the field where the EC of the soil is higher, with lower values in the middle-western part. Despite this, the values of the temperatures in T2 cannot be relied on, because the range of temperatures is too high, varying from 4.5 to 25 °C. However, the values in T4 seem more reliable, as they mainly range from 12.5 to 14.5 °C, but the pattern of the temperatures does not correspond with the one for the ECsat values.

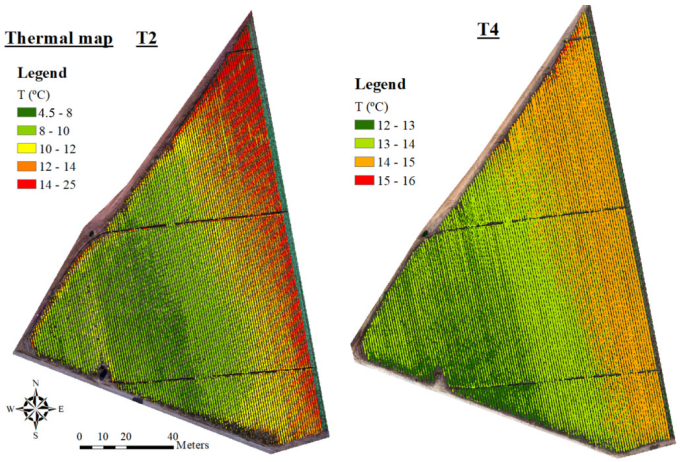

Figure 8. Thermal map of the vegetation for T2 and T4.

3.3.2. Normalized Difference Vegetative Index (NDVI)

The correlation between the ECsat and NDVI was insignificant for T3 and T4, but was moderately significant for T2, with an average R^2 of 0.29 for the whole sample. This is also evident in the maps in Figure 9, since the values of this vegetative index are fairly homogeneous over the whole field and do not seem to be related to the EC of the soil. The NDVI values grew, as predicted, over the growing season, reaching an average of 0.86 in T4.

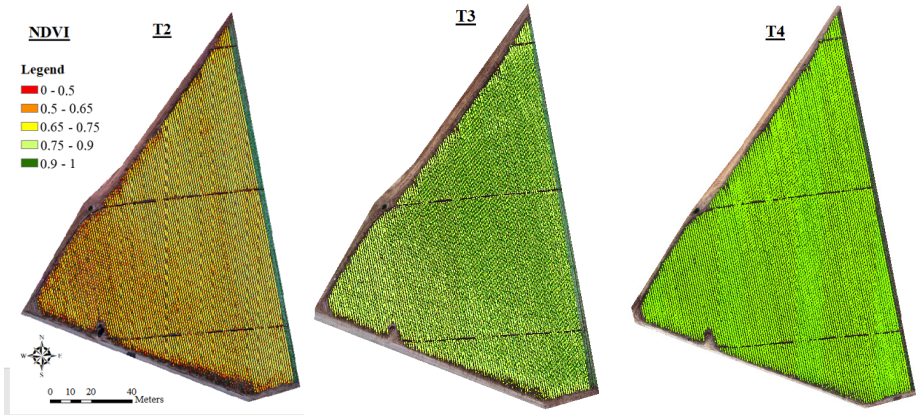

Figure 9. Map of the NDVI applied to vegetation for T2, T3, and T4.

3.3.3. Salinity Index (SI)

The SI exhibited a significant positive correlation with the ECsat for T2, an essentially reasonable correlation for T3 and T4, and an R^2 of 0.63 for the whole dataset using the following equation:

$$EC\_sat = (SI - 0.0158)/0.0946$$

The highest correlation in T2 was mostly attributable to the two samples with greater ECsat values, the same as for the canopy Ta, but with a correlation of the whole dataset that followed a similar trend as the T2, T3, and T4 samples. However, at first glance, the patterns shown for the ECsat values cannot be observed in the SI maps (Figure 10). The average SI between T2 and T3 fell from 0.12 to 0.06, as did the ECsat. The correlation was weaker for this sample because it grew from T3 to T4, while the ECsat continued to decline.

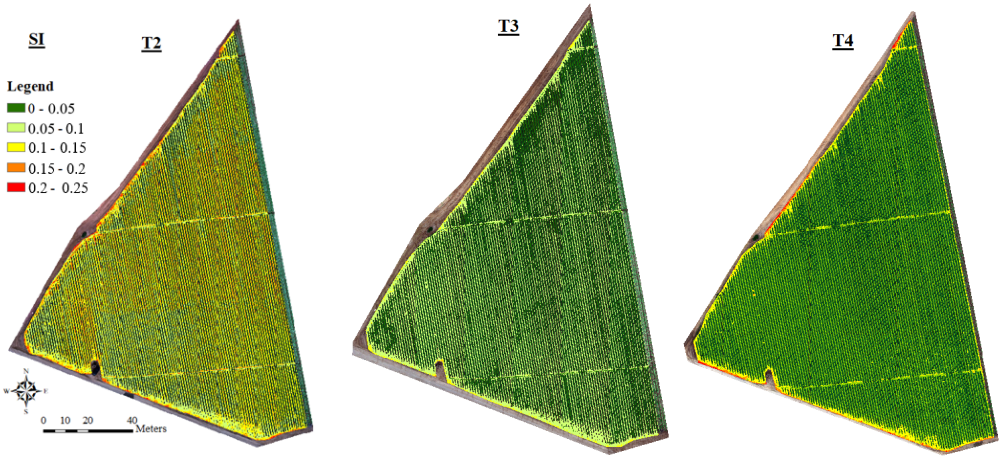

Figure 10. Map of the SI applied to bare soil for T2, T3, and T4.

3.3.4. Normalized Difference Salinity Index (NDSI)

For T2, T3, and T4, the NDSI showed insignificant correlations with the ECsat. Despite this, the correlation with the whole dataset was modest, with an R^2 of 0.52. This increased connection was due to the T4 values being significantly lower than in T2 and T3, and the correlation may not hold for a big sample with higher ECsat values. The average NDSI calculated from the maps (Figure 11) exhibited the same trend as the ECsat, decreasing steadily from −0.21 to −0.59 from T2 to T4 (being −0.51 in T3). However, the patterns shown in the ECsat images, particularly in T2, are not visible in the NDSI maps.

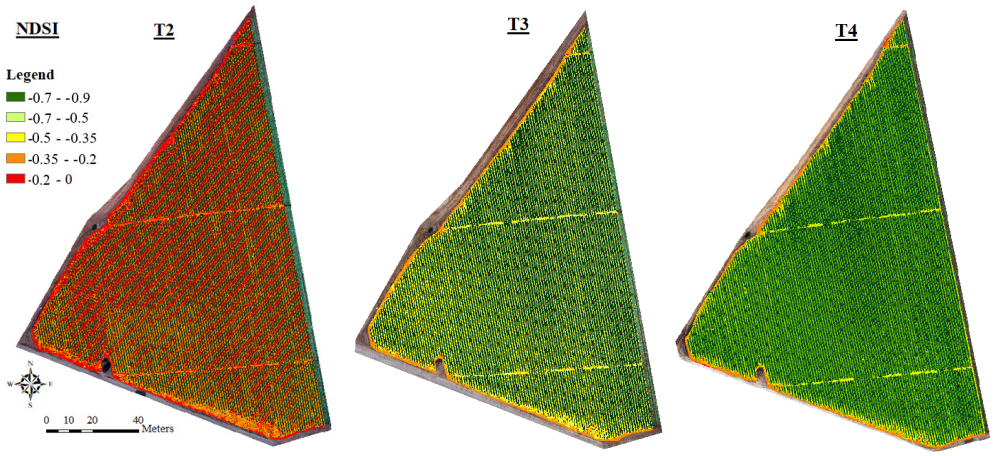

Figure 11. Map of the NDSI applied to bare soil for T2, T3, and T4.

4. Discussion

4.1. Crop Salt Tolerance

Lettuce is a sensitive crop to soil salts, with a threshold of 1.3 dS/m and a slope of 13% per dS/m [30,31]. As a result, there should have been yield losses of 43.68% in the SP and 28.73% in the CP. In the case of the commercial plot, there should have been no yield decrease owing to salinity, since the average ECsat was 39.23% lower than the criterion. In the next part we will go through the actual yields achieved in the experimental and commercial plots.

4.2. Crop Growth and Leaf Mineral Content

The lettuces in the commercial field, as well as those in the CP, flourished nicely. The ones in the SP, on the other hand, did not grow properly owing to mineral toxicity. The initial indication was a burning sensation in the leaf tips and edges, which was caused by chloride and salt toxicity [32], was obvious in the mineral content of the leaves, and was substantially greater in the SP lettuces than in the CP lettuces. Furthermore, the lettuces in the SP matured slower than those in the CP, which might have been due to ion nitrate toxicity, which slows the maturation process [32], which can also be assessed via the N/C ratio. The ratio was larger in the SP than in the CP, indicating that the cells in the CP were more developed. The ratios in the CP and commercial plots were quite close. These toxins were mostly derived from irrigation water and harmed the crop growth.

The lettuces cultivated in the SP were smaller and had more water than those grown in the CP. The expected difference of 14.95% between the CP and the SP production was close to the findings, as the fresh and dried lettuce heart weights were 18.72% and 9.26% greater in the CP, respectively. Furthermore, the commercial plot lettuces should not have shown any yield drop; however, the CP lettuces should have been 28.73% lower, which was extremely comparable to the difference (of 29.65%) reported in the dry lettuce weight. Other investigations found comparable variations between lettuces irrigated with ECws, ranging from 0.9 to 3.6 dS/m. The water content in the lettuces produced under comparable circumstances was found to be almost same [31], or 0.73% higher in the control treatment [33].

Inside the greenhouse, the temperature and relative humidity were ideal for the growth of the fungus Sclerotinia sclerotiorum, which has a maximum mycelial growth temperature of 20 °C and a relative humidity of 90% [34]. The fungicide affected many lettuces in the SP but just a few in the CP. Although previous research found that the pathogen growth decreased as the salinity increased [35–37], it is possible that there were more sclerotia (specialized resistant survival structures) in this part of the field, which can live for up to 8 years in the soil [35,36].

However, there were certain factors that were very high or extremely low. There was a deficiency of calcium, magnesium, and iron in the experimental SP, and a likely toxicity of Cu, since the levels discovered were four times (or more) greater than in the prior study. The symptoms of these deficiencies and toxicity [37,38] correlate with those reported for lettuces, particularly the SP, such as leaf curling owing to a calcium shortfall. At harvest, the mineral concentrations of various elements, such as potassium, phosphorus, calcium, iron, and magnesium, were low in the commercial plot. The lettuces, on the other hand, showed no signs. The fact that the levels of iron in the commercial and experimental plots were quite high before harvesting might have been because this element tends to concentrate in the old and exterior leaves, which were not analyzed at harvest (only the lettuce heart was).

4.3. Canopy Temperature

The canopy temperature in T2 in the greenhouse plot was on average 1.4 °C higher for lettuces grown in the SP compared to those planted in the CP, whereas some authors [27] reported lesser differences (0.88–1.19 °C) in China when cultivating alfalfa under moderate to severe saline conditions compared to no salinity. Because lettuce is more sensitive to soil salts than alfalfa, the temperature differential is greater. The T2 temperature values

observed in the experimental plot were comparable to those discovered in earlier studies performed with lettuce under greenhouse settings in Argentina and Germany, with values ranging from 21 to 25 °C [39,40]. The extremely low R^2 values observed in T2 and T3 might be explained by issues with the thermal camera, as well as the fact that in T3 the temperatures in the SP were lower than in the CP due to the high air humidity, meaning we were also unable to generate a map from the photos.

The findings obtained in T2 in the commercial plot were moderately associated with the ECsat, with an R^2 of 0.5, which was a stronger correlation than that found by Ivushkin et al. (2019) in quinoa (a salt-resistant crop) following NDVI clustering in the Netherlands [41]. However, without NDVI clustering, the differences between the control quinoa plot and the saline plot, with an ECsat over 30 dS/m, were not substantially different in the newest research, and it was indicated that crops sensitive to salts would have bigger temperature differences under saline circumstances. The findings in this thesis support the assumption that a less tolerant crop would exhibit more temperature variations and so have better correlations [27,28]. Furthermore, the patterns for the canopy Ta and ECsat in T2 were quite similar, as reported in previous research [42]; however, the temperature values discovered cannot be relied on, as a temperature variation of approximately 20 °C in around 1 ha under somewhat saline circumstances is not plausible. The temperatures and range recorded in T4 seem more trustworthy, as the temperature of the lettuce leaves begins to approach the ambient temperature [36]. More studies using a thermal camera under ideal weather circumstances should be conducted to discover whether the relationships are stronger and the values more dependable.

4.4. NDVI

Several prior studies employed vegetative indicators and discovered considerable connections with the soil salinity [43–45]. However, the relationships between the NDVI and ECsat in this research were insignificant. In the greenhouse plot, the differences between the SP and CP were greatest early on, and there was almost no difference before them at harvest. A similar trend occurred in the commercial plot, where the largest linear correlation was 0.32 in T2, followed by minor differences. Similar low correlations where presented [42] when comparing the NDVI values recorded in quinoa, a salt-tolerant crop, in non-saline and extremely severe saline environments (over 30 dS/m). Furthermore, a group of researchers [46] created a model to predict the EC of soil in Ethiopia in a semi-arid environment, using several vegetal and soil indices, and the NDVI performed the worst, with an R^2 of 0.002. However, research performed in Iran using sugarcane [17], a salt-sensitive crop with a comparable soil salinity threshold to lettuce, discovered a modest positive connection (R^2 = 0.68) between the NDVI and ECsat. Another study found [47] modest connections in arid and semi-arid environments across a vast region in Iran, with an R^2 value of 0.58. Based on the prior research, a greater connection could be predicted for a salt-sensitive crop such as lettuce, although the saline plot should have a higher EC to reveal significant differences with the control plot, or it should be applied to the vegetation and bare soil rather than just the vegetation. It would be interesting to further investigate this index to see whether it might be used by farmers to measure soil EC values.

4.5. SI

The SI had high and moderate correlations with the ECsat, both in the experimental and commercial plots. The R^2 values ranged from 0.74 to 0.80 in the experimental plot, with a value of 0.83 for the whole dataset, and from 0.4 to 0.75 in the commercial plot, with a value of 0.63 for the whole dataset. Moreover, the correlations of the samples taken between the ridges in the CP and SP also showed moderate linear correlation of 0.65. Similar results were found in previous studies. In 2017, researchers [22] monitored the soil salinity in a salty lake and its surroundings in Turkey, obtaining a correlation of 0.77. Moreover, in another study conducted in a large agricultural plain in Morocco [48], a moderate correlation (R^2 = 0.55) was found between the SI and ECsat. However, when the SI was

applied in very strongly saline soils, [19] obtained negligible and low correlations in an oasis dominated by date palm plants in Arabia Saudi; possibly the scatter plot placed most of the samples in a group with a very high salinity, and the correlation was lower because of this. A previous study [46] performed in an irrigated sugar cane farm in Ethiopia obtained a correlation of 0.63, using a similar equation to the one obtained for the commercial plot. The lack of scatterplots and equations in the other studies that researched the SI makes it difficult to contrast the values obtained, but the ones found in the experimental plot seemed too low. Furthermore, the SI was only applied to bare soil in this thesis, which might be one of the reasons why the correlation was higher than in other studies. More research should be performed to find the best formula to predict the ECsat from the SI, which will increase the quality of the assessments of soil salinity, avoid the need to analyze soil samples, and save farmers time and money.

4.6. NDSI

The correlation of the NDSI and ECsat was negligible in the commercial plot for each sample and low in the experimental plot, despite the fact that the overall dataset correlations were low or moderate in both cases, with linear correlations of 0.49 and 0.52 in the experimental and commercial plots, respectively. The findings of prior large-scale investigations were comparable. Researchers found [46] a correlation of 0.39 in an irrigated sugar cane region in Ethiopia, with ECsat values ranging between 0 and 6 dS/m, and under extremely highly saline conditions a moderate correlation (R^2 = 0.32) was discovered in arid and semi-arid regions in Abu Dhabi [49] and an oasis in Saudi Arabia [19]. However, the projected values for a certain ECsat varied between the result found in earlier research and those observed in this study. For example, the from researchers [46] anticipated an NDSI value of 0.4 for an ECsat measurement of roughly 1 dS/m, while others [49] found an NDSI value of −0.08, and in the present article the commercial plot showed a value of −0.65, while the experimental plot's value was −0.24. These variations might be due to the fact that the same index was employed in various climatic and soil conditions, as well as being applied to plants, bare soil, or both. More studies, including scatterplots and equations to forecast the ECsat, are needed to evaluate whether it is a good indicator for assessing soil salinity in agricultural areas and to identify its limits.

5. Conclusions

In our analysis, saline irrigation water had detrimental impacts on the crop growth and leaf mineral content. The lettuces grown in saltwater environments were impacted by mineral deficiency or toxicity, resulting in delayed development, wrinkled leaves, and burnt tips. The components in the irrigation water influenced the mineral composition of the leaves, with the SP having almost double the quantities of chloride and sodium as the CP. At harvest, the fresh head weight in the CP was 18% greater than in the SP, with no variation in head diameter or height.

When the thermal camera was utilized under ideal weather circumstances, the canopy Ta produced encouraging findings, with a moderate linear correlation of R^2 = 0.5 and a similar visual pattern as for soil salinity. The second vegetative parameter, NDVI, exhibited minimal correlations and no visible differences other than the reduced size of the lettuces produced in the SP compared to those growing in the CP during the beginning stages. The soil salinity indicators, the SI and NDSI, displayed greater correlations than the NDVI; however, the soil salinity patterns could not be separated. The SI fared the best of all the measures, with the linear correlations ranging from 0.63 to 0.83. As in the earlier investigations, excellent findings were achieved, and it can be concluded that the SI is a promising measure for predicting soil salinity with high accuracy. Furthermore, as compared to the earlier research, the strong correlations observed with the canopy Ta support the idea that the correlations with the soil salinity would be larger with a crop more sensitive to the salts in the soil. As a result, additional studies should be conducted in dry or semi-arid environments using lettuce in a flat planting arrangement or another sensitive

crop to create equations capable of predicting soil salinity from thermal and multispectral camera data.

Author Contributions: Conception and design of the study: F.P.S., P.P.C., A.T.; acquisition of the data: P.P.C.; analysis and interpretation of the data:, F.A., F.P.S., P.P.C., M.L.E., H.B. (Harm Boesveld), H.B. (Harm Bartholomeus); drafting of the manuscript: F.P.S., P.P.C., M.L.E.; critical revision of the manuscript for important intellectual content: F.P.S., P.P.C., A.T., M.L.E.; approval of the version of the manuscript to be published: F.P.S., P.P.C., M.L.E., H.B. (Harm Boesveld), H.B. (Harm Bartholomeus). All authors have read and agreed to the published version of the manuscript.

Funding: RYC2020-030356-I and project CICLICA (PCI2022-132959), funded by MCIN/AEI/10.13039/501100011033 and the EU "NextGenerationEU"/PRTR".

Informed Consent Statement: Not applicable.

Data Availability Statement: Not applicable.

Acknowledgments: RYC2020-030356-I and project CICLICA (PCI2022-132959), funded by MCIN/AEI/10.13039/501100011033 and the EU "NextGenerationEU"/PRTR".

Conflicts of Interest: The authors declare no conflict of interest.

References

1. United Nations, Department of Economic and Social Affairs, Population Division. *World Population Prospects: The 2017 Revision, Key Findings and Advance Tables*; Working Paper No. ESA/P/WP/248; United Nations, Department of Economic and Social Affairs, Population Division: New York, NY, USA, 2017.
2. Drechsel, P.; Qadir, M.; Wichelns, D. (Eds.) *Wastewater Economic Asset in Urbanizing World*; Springer: Dordrecht, The Netherlands, 2015. [CrossRef]
3. Jaramillo, M.; Restrepo, I. Wastewater Reuse in Agriculture: A Review about Its Limitations and Benefits. *Sustainability* **2017**, *9*, 1734. [CrossRef]
4. Reichel, A.; Lazarova, M. The Effects of Outsourcing and Devolvement on the Strategic Position of HR Departments: Outsourcing, Devolvement, and Strategic Position of HR Departments. *Hum. Resour. Manag.* **2013**, *52*, 923–946. [CrossRef]
5. Vivaldi, G.A.; Camposeo, S.; Rubino, P.; Lonigro, A. Microbial impact of different types of municipal wastewaters used to irrigate nectarines in Southern Italy. *Agric. Ecosyst. Environ.* **2013**, *181*, 50–57. [CrossRef]
6. Norton-Brandão, D.; Scherrenberg, S.M.; van Lier, J.B. Reclamation of used urban waters for irrigation purposes—A review of treatment technologies. *J. Environ. Manag.* **2013**, *122*, 85–98. [CrossRef]
7. Parsons, L.R.; Sheikh, B.; Holden, R.; York, D.W. Reclaimed Water as an Alternative Water Source for Crop Irrigation. *HortScience* **2010**, *45*, 1626–1629. [CrossRef]
8. Pedrero, F.; Alarcón, J.J.; Nicolás, E.; Mounzer, O. Influence of irrigation with saline reclaimed water on young grapefruits. *Desalination Water Treat.* **2013**, *51*, 2488–2496. [CrossRef]
9. Martínez, S.; Suay, R.; Moreno, J.; Segura, M.L. Reuse of tertiary municipal wastewater effluent for irrigation of *Cucumis melo* L. *Irrig. Sci.* **2013**, *31*, 661–672. [CrossRef]
10. Pedrero, F.; Kalavrouziotis, I.; Alarcón, J.J.; Koukoulakis, P.; Asano, T. Use of treated municipal wastewater in irrigated agriculture—Review of some practices in Spain and Greece. *Agric. Water Manag.* **2010**, *97*, 1233–1241. [CrossRef]
11. Tallou, A.; Haouas, A.; Jamali, M.Y.; Atif, K.; Amir, S.; Aziz, F. Review on Cow Manure as Renewable Energy. In *Smart Village Technology*; Patnaik, S., Sen, S., Mahmoud, M.S., Eds.; Modeling and Optimization in Science and Technologies; Springer International Publishing: Cham, Switzerland, 2020; Volume 17, pp. 341–352. ISBN 978-3-030-37793-9. [CrossRef]
12. Tallou, A.; Aziz, F.; Garcia, A.J.; Salcedo, F.P.; El Minaoui, F.E.; Amir, S. Bio-fertilizers issued from anaerobic digestion for growing tomatoes under irrigation by treated wastewater: Targeting circular economy concept. *Int. J. Environ. Sci. Technol.* **2021**, *19*, 2379–2388. [CrossRef]
13. Xu, M.; Bai, X.; Pei, L.; Pan, H. A research on application of water treatment technology for reclaimed water irrigation. *Int. J. Hydrogen Energy* **2016**, *41*, 15930–15937. [CrossRef]
14. Dickin, S.K.; Schuster-Wallace, C.J.; Qadir, M.; Pizzacalla, K. A Review of Health Risks and Pathways for Exposure to Wastewater Use in Agriculture. *Environ. Health Perspect.* **2016**, *124*, 900–909. [CrossRef] [PubMed]
15. Karthikeyan, L.; Chawla, I.; Mishra, A.K. A review of remote sensing applications in agriculture for food security: Crop growth and yield, irrigation, and crop losses. *J. Hydrol.* **2020**, *586*, 124905. [CrossRef]
16. Salcedo, F.P.; Cutillas, P.P.; Cabañero, J.J.A.; Vivaldi, A.G. Use of remote sensing to evaluate the effects of environmental factors on soil salinity in a semi-arid area. *Sci. Total Environ.* **2022**, *815*, 152524. [CrossRef] [PubMed]
17. Hamzeh, S.; Naseri, A.A.; Alavipanah, S.K.; Mojaradi, B.; Bartholomeus, H.M.; Clevers, J.G.; Behzad, M. Estimating salinity stress in sugarcane fields with spaceborne hyperspectral vegetation indices. *Int. J. Appl. Earth Obs. Geoinf.* **2013**, *21*, 282–290. [CrossRef]

18. Nawar, S.; Buddenbaum, H.; Hill, J.; Kozak, J. Modeling and Mapping of Soil Salinity with Reflectance Spectroscopy and Landsat Data Using Two Quantitative Methods (PLSR and MARS). *Remote Sens.* **2014**, *6*, 10813–10834. [CrossRef]
19. Allbed, A.; Kumar, L.; Aldakheel, Y.Y. Assessing soil salinity using soil salinity and vegetation indices derived from IKONOS high-spatial resolution imageries: Applications in a date palm dominated region. *Geoderma* **2014**, *230–231*, 1–8. [CrossRef]
20. Bai, L.; Wang, C.; Zang, S.; Zhang, Y.; Hao, Q.; Wu, Y. Remote Sensing of Soil Alkalinity and Salinity in the Wuyu'er-Shuangyang River Basin, Northeast China. *Remote Sens.* **2016**, *8*, 163. [CrossRef]
21. El Harti, A.; Lhissou, R.; Chokmani, K.; Ouzemou, J.; Hassouna, M.; Bachaoui, E.M.; El Ghmari, A. Spatiotemporal monitoring of soil salinization in irrigated Tadla Plain (Morocco) using satellite spectral indices. *Int. J. Appl. Earth Obs. Geoinf.* **2016**, *50*, 64–73. [CrossRef]
22. Gorji, T.; Sertel, E.; Tanik, A. Monitoring soil salinity via remote sensing technology under data scarce conditions: A case study from Turkey. *Ecol. Indic.* **2017**, *74*, 384–391. [CrossRef]
23. Romero-Trigueros, C.; Nortes, P.A.; Alarcón, J.J.; Hunink, J.E.; Parra, M.; Contreras, S.; Droogers, P.; Nicolás, E. Effects of saline reclaimed waters and deficit irrigation on Citrus physiology assessed by UAV remote sensing. *Agric. Water Manag.* **2017**, *183*, 60–69. [CrossRef]
24. Gómez-Bellot, M.J.; Ortuño, M.F.; Nortes, P.A.; Vicente-Sánchez, J.; Bañón, S.; Sánchez-Blanco, M.J. Mycorrhizal euonymus plants and reclaimed water: Biomass, water status and nutritional responses. *Sci. Hortic.* **2015**, *186*, 61–69. [CrossRef]
25. Quebrajo, L.; Perez-Ruiz, M.; Pérez-Urrestarazu, L.; Martínez, G.; Egea, G. Linking thermal imaging and soil remote sensing to enhance irrigation management of sugar beet. *Biosyst. Eng.* **2018**, *165*, 77–87. [CrossRef]
26. Ivushkin, K.; Bartholomeus, H.; Bregt, A.K.; Pulatov, A.; Kempen, B.; de Sousa, L. Global mapping of soil salinity change. *Remote Sens. Environ.* **2019**, *231*, 111260. [CrossRef]
27. Tian, F.; Hou, M.; Qiu, Y.; Zhang, T.; Yuan, Y. Salinity stress effects on transpiration and plant growth under different salinity soil levels based on thermal infrared remote (TIR) technique. *Geoderma* **2020**, *357*, 113961. [CrossRef]
28. Gartley, K.L. Recommended Methods for Measuring Soluble Salts in Soils. In *Recommended Soil Testing Procedures for the Northeastern United States*; Cooperative Bulletin No. 493; University of Delaware: Newark, DE, USA, 2011; pp. 87–94.
29. Hammer, O.; Harper, D.A.T.; Ryan, P.D. PAST: Paleontological Statistics Software Package for Education and Data Analysis. *Palaeontol. Electron.* **2001**, *4*, 9.
30. Bernstein, L.; Francois, L.E.; Clark, R.A. Interactive Effects of Salinity and Fertility on Yields of Grains and Vegetables. *Agron. J.* **1974**, *66*, 412–421. [CrossRef]
31. Lara, M.; Diezma, B.; Lleó, L.; Roger, J.; Garrido, Y.; Gil, M.; Ruiz-Altisent, M. Hyperspectral Imaging to Evaluate the Effect of IrrigationWater Salinity in Lettuce. *Appl. Sci.* **2016**, *6*, 412. [CrossRef]
32. Ayers, R.S.; Westcot, D.W. *Water Quality for Agriculture*; FAO: Rome, Italy, 1985.
33. Ahmed, S.; Ahmed, S.; Roy, S.K.; Woo, S.H.; Sonawane, K.D.; Shohael, A.M. Effect of salinity on the morphological, physiological and biochemical properties of lettuce (*Lactuca sativa* L.) in Bangladesh. *Open Agric.* **2019**, *4*, 361–373. [CrossRef]
34. Krishnamoorthy, K.K.; Sankaralingam, A.; Nakkeeran, S. Effect of Temperature and Salinity on the Growth of Sclerotinia sclerotiorum Causing Head Rot of Cabbage. *Int. J. Curr. Microbiol. Appl. Sci.* **2017**, *6*, 950–954. [CrossRef]
35. Abdullah, M.T.; Ali, N.Y.; Suleman, P. Effect of Salinity, Temperature and Carbon Source on the Growth and Development of Sclerotia of Sclerotinia sclerotiorum Isolated from Semi-arid Environment. *Plant Pathol. J.* **2008**, *24*, 407–416. [CrossRef]
36. Silva, S.; do Nascimento, R.; Oliveira, H.; Cardoso, J.A.F.; Xavier, D.A.; de Sousa Silva, S.; Silva, S.; do Nascimento, R.; Oliveira, H.; Cardoso, J.A.F.; et al. Levels of nitrate, pigments and thermographic analysis of lettuce under different temperatures of nutrient solution. *Afr. J. Agric. Res.* **2016**, *11*, 1668–1673. [CrossRef]
37. Smolinska, U.; Horbowicz, M. Fungicidal Activity of Volatiles from Selected Cruciferous Plants against Resting Propagules of Soil!borne Fungal Pathogens. *Blackwell Wiss.-VerlagBerlin* **1999**, *147*, 119–124. [CrossRef]
38. Talib Alkooranee, J.; Raad Aledan, T.; Xiang, J.; Lu, G.; Li, M. Induced Systemic Resistance in Two Genotypes of Brassica napus (AACC) and Raphanus oleracea (RRCC) by Trichoderma Isolates against Sclerotinia sclerotiorum. *Am. J. Plant Sci.* **2015**, *6*, 1662–1674. [CrossRef]
39. Simon, E.W. The Symptoms of Calcium Deficiency in Plants. *New Phytol.* **1978**, *80*, 1–15. [CrossRef]
40. Inmaculada, Y. Copper in Plants. *Toxic Met. Plant* **2005**, *17*, 145–156.
41. Sandmann, M.; Grosch, R.; Graefe, J. The Use of Features from Fluorescence, Thermography, and NDVI Imaging to Detect Biotic Stress in Lettuce. *Plant Dis.* **2018**, *102*, 1101–1107. [CrossRef]
42. Ivushkin, K.; Bartholomeus, H.; Bregt, A.K.; Pulatov, A. Satellite Thermography for Soil Salinity Assessment of Cropped Areas in Uzbekistan. *Land Degrad. Dev.* **2017**, *28*, 870–877. [CrossRef]
43. Aldakheel, Y.Y.; Elprince, A.M.; Aatti, M.A. Mapping Vegetation and Saline Soil Using NDVI in Arid Irrigated Lands. In Proceedings of the ASPRS 2006 Annual Conference, Reno, NV, USA, 1–5 May 2006.
44. Brunner, P.; Li, H.T.; Kinzelbach, W.; Li, W.P. Generating soil electrical conductivity maps at regional level by integrating measurements on the ground and remote sensing data. *Int. J. Remote Sens.* **2007**, *28*, 3341–3361. [CrossRef]
45. Platonov, A.; Noble, A.; Kuziev, R. Soil Salinity Mapping Using Multi-Temporal Satellite Images in Agricultural Fields of Syrdarya Province of Uzbekistan. In *Developments in Soil Salinity Assessment and Reclamation*; Shahid, S.A., Abdelfattah, M.A., Taha, F.K., Eds.; Springer: Dordrecht, The Netherlands, 2013; pp. 87–98. ISBN 978-94-007-5683-0.

46. Asfaw, E.; Suryabhagavan, K.V.; Argaw, M. Soil salinity modeling and mapping using remote sensing and GIS: The case of Wonji sugar cane irrigation farm, Ethiopia. *J. Saudi Soc. Agric. Sci.* **2018**, *17*, 250–258. [CrossRef]
47. Hammam, A.A.; Mohamed, E.S. Mapping soil salinity in the East Nile Delta using several methodological approaches of salinity assessment. *Egypt. J. Remote Sens. Space Sci.* **2020**, *23*, 125–131. [CrossRef]
48. Bachaoui, B.; Bachaoui, E.M.; Maimouni, S.; Lhissou, R.; El Harti, A.; El Ghmari, A. The use of spectral and geomorphometric data for water erosion mapping in El Ksiba region in the central High Atlas Mountains of Morocco. *Appl. Geomat.* **2014**, *6*, 159–169. [CrossRef]
49. Abuelgasim, A.; Ammad, R. Mapping soil salinity in arid and semi-arid regions using Landsat 8 OLI satellite data. *Remote Sens. Appl. Soc. Environ.* **2019**, *13*, 415–425. [CrossRef]